Chapter 2 Synthesis and Characterization Techniques

This chapter deals with the description of the research facilities used for the synthesis and characterization of different MoS_2 nanostructures over Si and SiO_2/Si substrates for photodetector and SERS applications. In the present work, three different MoS_2 nanostructures have been prepared via chemical vapour deposition (CVD) technique and growth mechanism for different morphologies has been discussed in this chapter. Fundamentals related to different characterization techniques like XRD, SEM, Raman, Photoluminescence and UV-visible absorption spectroscopy have been discussed in this chapter.

2.1 Materials Synthesis

The 2D materials can be synthesized by two approaches- top-down and bottom-up, as shown schematically in **Figure 2.1**. The widely used top-down approach incudes mechanical exfoliation, liquid phase exfoliation and Lithium-ion intercalation methods [36-38]. These exfoliation processes are suitable for synthesis of 2D materials due to the presence of weak van der Waal force between the layers, that allows individual 2D layers to be separated from its bulk counterpart. However, growing large area homogeneous 2D MoS_2 film remains a challenge using these methods. On the other hand, bottom-up approach can be used to synthesize homogeneous 2D nanostructures. This approach includes the physical vapor deposition (PVD), chemical vapor deposition (CVD) and solution chemical (hydrothermal/solvothermal) process. In the present work, three different morphologies of 2D MoS_2 nanostructures have been synthesized over Si and SiO_2/Si substrates using CVD technique. Three different morphologies of MoS_2 prepared in the present work are as follows-

a) Horizontally interconnected network of few-layer MoS_2 over Si substrate

b) Horizontally grown triangular bi-layer MoS_2 over SiO_2/Si substrate

c) Vertically oriented few-layer (VFL) MoS_2 over Si substrate

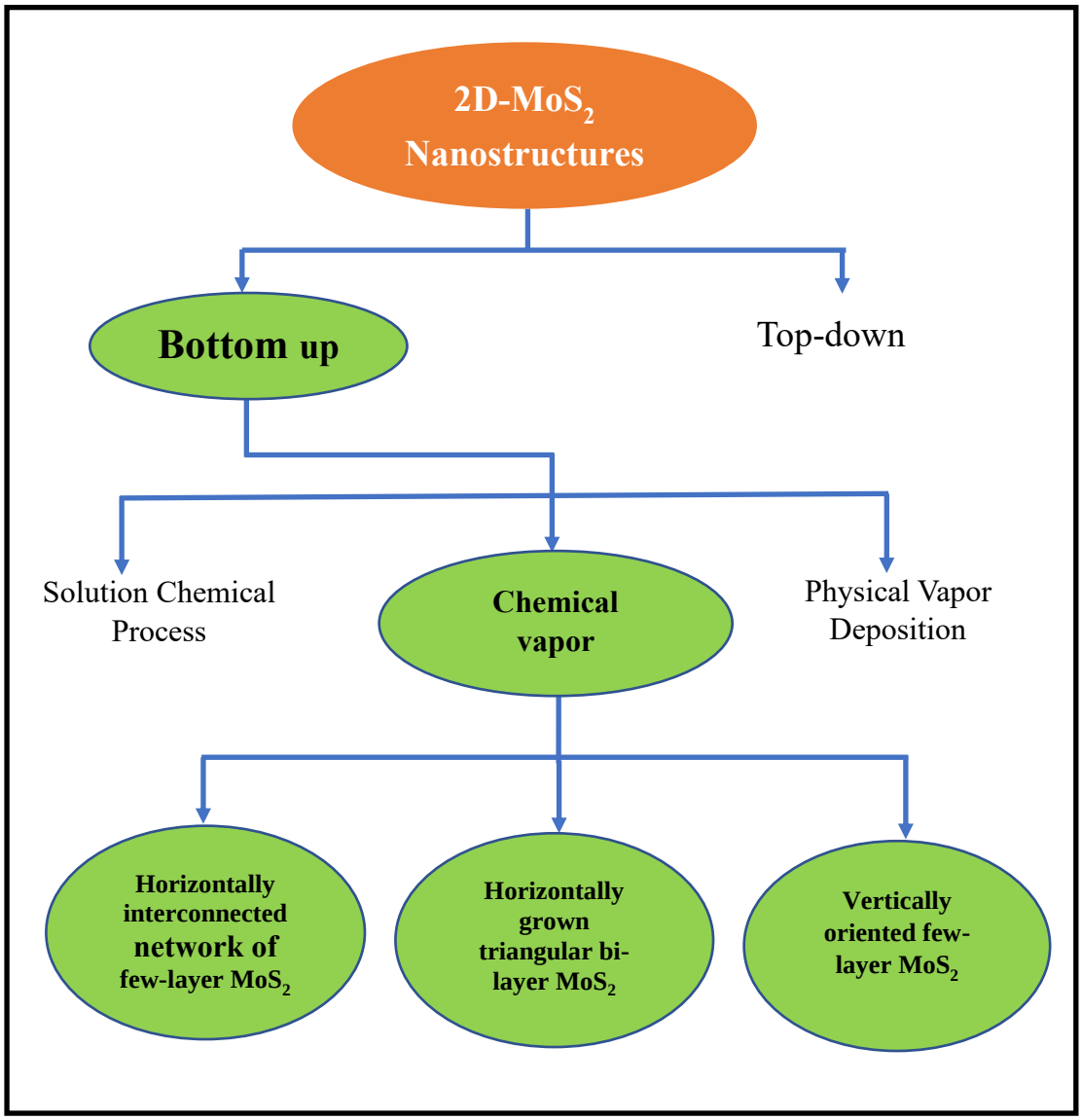

Figure 2.1 *Schematic diagram of synthesis process for 2D-MoS_2 nanostructures.*

2.1.1 CVD Synthesis of MoS_2 Nanostructures

In CVD process, chemical reactions take place among different precursors on and near the hot surfaces, resulting in the deposition of a thin film on the surface. The schematic diagram of CVD process for the growth of MoS_2 nanostructures is shown in

Figure 2.2. It consists of different components like quartz tube, heating coil and vacuum pump. The kinetics and thermodynamics of the chemical process plays a crucial role in growth of 2D materials. Tuning the amount of precursors, gas flow rate, reaction temperature and heating rate can lead to different kinetic and thermodynamic behaviour, which can result in different morphologies of MoS_2 nanostructures [128, 129].

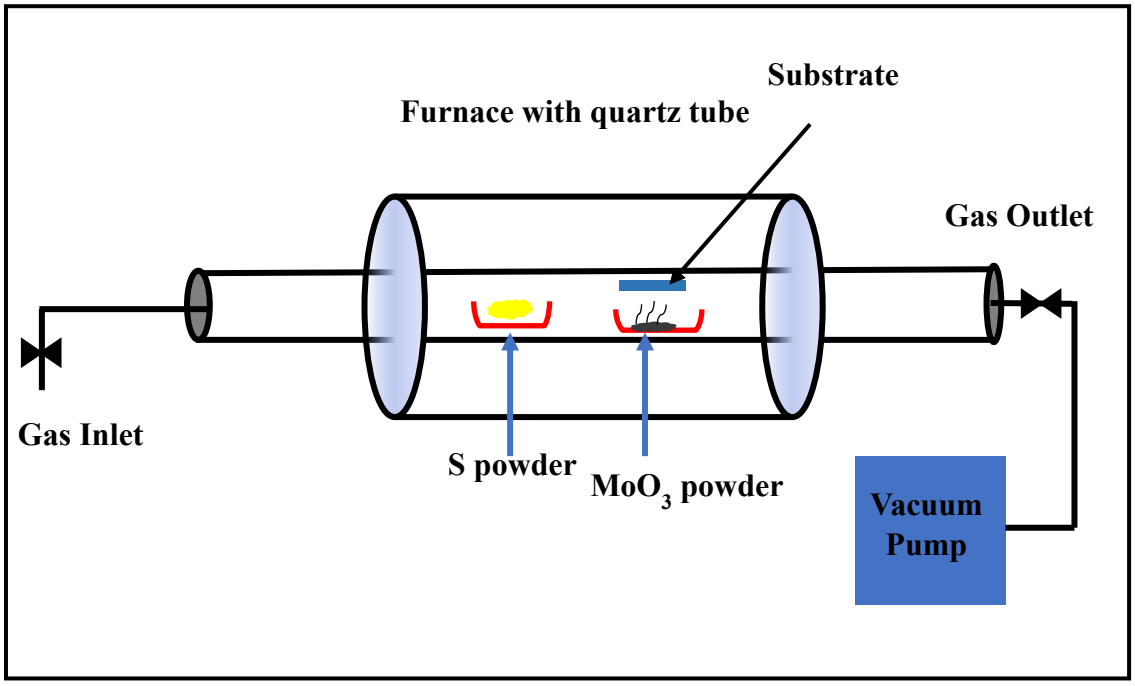

Figure 2.2 *Schematic diagram of MoS_2 growth via CVD method.*

In the present work, three different morphologies of MoS_2 nanostructures have been prepared over Si and SiO_2/Si substrates. We have used MoO_3 and sulphur powder as a precursor and nitrogen gas as a carrier gas for the synthesis of all the MoS_2 film [130]. The following chemical reactions take place at reaction temperature during synthesis of MoS_2 in CVD process [130,131]-

$$MoO_3 + x/2\ S \rightarrow MoO_{3-x} + x/2\ SO_2 \quad (2.1)$$

$$MoO_{3-x} + (7-x)/2\ S \rightarrow MoS_2 + (3-x)/2\ SO_2 \quad (2.2)$$

where MoO_2 is intermediate phase formed when x = 1, and the MoO_3 is reduced by the sulphur[130, 131]. The specific control of edge geometry is significant for their

applications in nanoelectronics and catalysis. The experimental condition of growth of different morphology of prepared MoS_2 nanostructures is shown in **Figure 2.3**. In CVD process, different parameters like temperature, chemical potential, vapour pressure, distance between the substrate and the precursors etc. can be tuned to achieve different shapes, size and morphologies of the desired material [132, 133]. The following sections provide the details of synthesis of three morphologies of MoS_2 nanostructures.

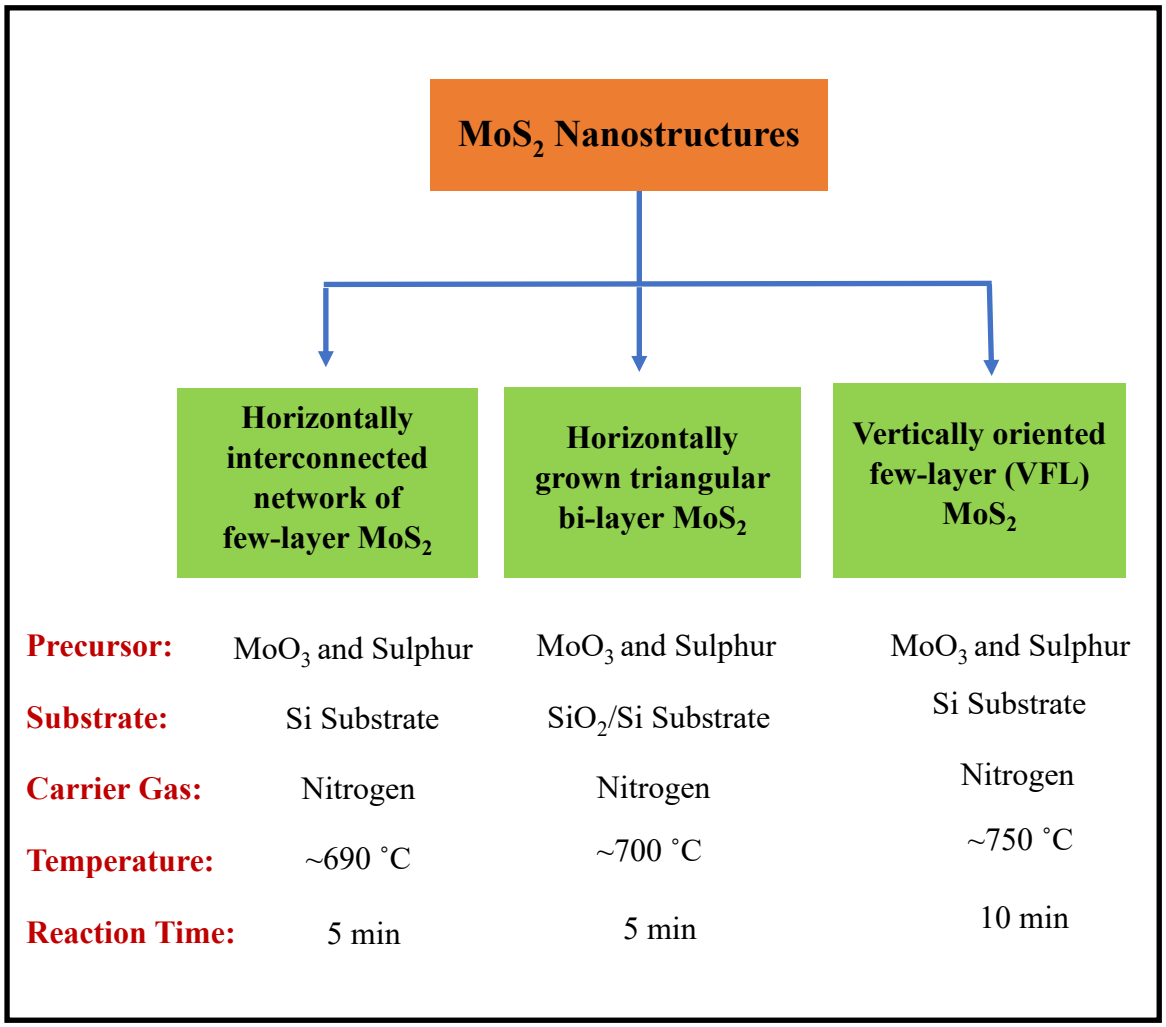

Figure 2.3 *Schematic diagram of experimental condition of synthesis of different morphologies of 2D-MoS_2 nanostructures.*

2.1.1.1 Horizontally Grown Interconnected Network Few-Layer MoS_2 Nanostructure

Horizontal interconnected network MoS_2 nanostructure over p-type Si substrate was synthesized by CVD technique. The Si substrate was placed just over the MoO_3 powder inside the quartz boat. Initially, the vacuum was created in the quartz tube before filling with N_2 gas with a flow rate of 100 sccm. The furnace was heated up to 690 °C at 10 °C/min heating rate and the reaction was performed around 5 min. At initial stage of reaction, formation of nucleation sites on Si substrate took place. Then the MoO_3 powder was reduced by the sulphur according to the **equation 2.1** and **2.2** to form MoS_2 nanostructures. Finally, the furnace was allowed to cool to room temperature at a natural rate.

2.1.1.2 Horizontally Grown Triangular Bi-Layer MoS_2 Nanostructure

The triangular bi-layer MoS_2 nanostructure was prepared on SiO_2/Si substrate via CVD method using MoO_3 and sulphur powder. The reaction was performed at 700 °C for 5 min in N_2 atmosphere with gas flow rate of 100 sccm and heating rate of 10 °C/min. The growth mechanism of triangular shaped MoS_2 is shown schematically in **Figure 2.4**. At initial state of reaction, formation of nucleation sites on the SiO_2/Si substrate takes place in large number. As substrate is placed on the top of MoO_3, the partial pressure of MoO_3 vapour is higher as compared to sulphur vapour and dodecagonal shape is formed initially due to Molybdenum rich condition. The partial pressure of sulphur powder gradually increases during growth process and once the stoichiometric ratio of Mo:S (1:2) is achieved hexagonal shape is formed, which is further distorted with increasing sulphur concentration and yield triangular shape in rich sulphur condition, as shown schematically in **Figure 2.4** on the basis of Wulf construction rule [133]. The equivalent shape of MoS_2 can be determined by this rule once the formation energies of arbitrary

edges are achieved. The fast-growing faces are found smaller in size compared to slowest growing faces. The surface free energy plays a crucial role in determining the growth rate of phases in 2D materials and the low energy phases grow slowly [132]. The synthesized bi-layer MoS_2 over SiO_2/Si is equilateral triangle flake with different sizes in the range 10-20 μm.

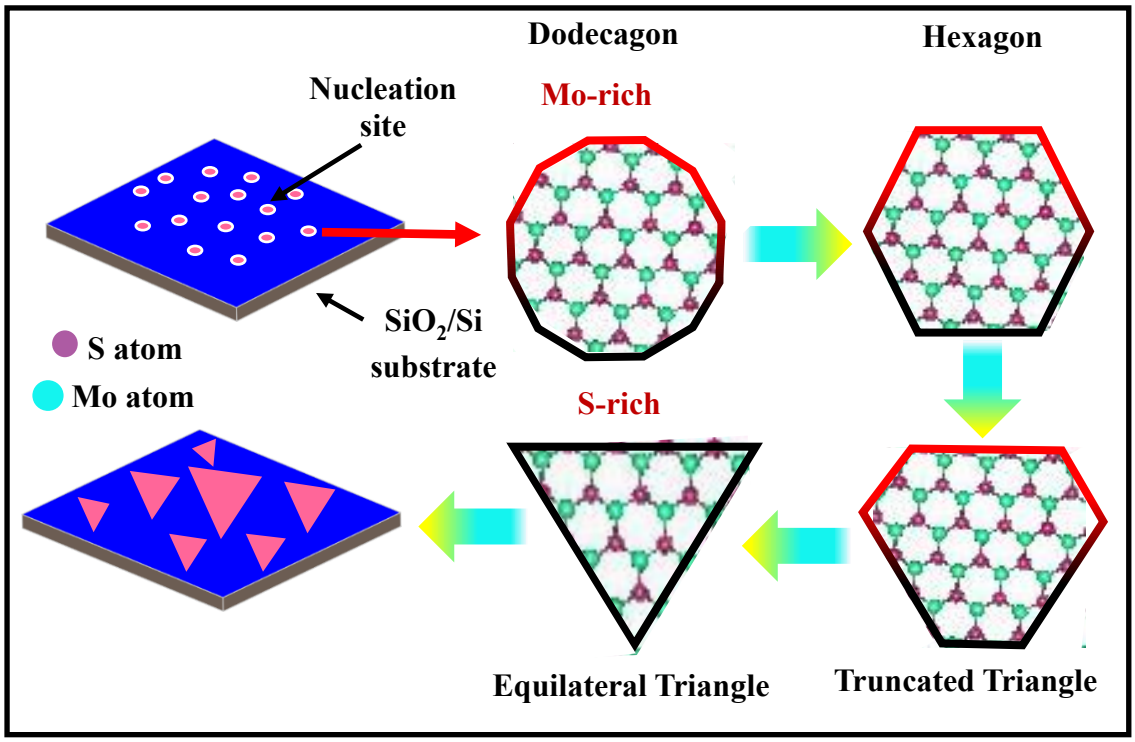

Figure 2.4 *Schematic diagram of growth mechanism of triangular bi-layer MoS_2 nanostructure over SiO_2/Si substrate.*

2.1.1.3 Vertically Grown Few-Layer MoS_2 Nanostructure

We also showed the growth of vertically oriented few-layer (VFL) MoS_2 nanosheets over large area (1×1 cm^2) of Si substrates via CVD method. The reaction process was performed at 750 °C for 10 min under N_2 atmosphere with gas flow rate of 100 sccm. The high density of nucleation sites due to large amount of MoO_3 and larger growth time tends to merge 2D MoS_2 films in the vertical direction to the Si substrate. The schematic representation for growth mechanism of VFL MoS_2 is shown in **Figure**

2.5. The sulphur vapor partially reduces the MoO_3 powder to form volatile MoO_{3-x} or gaseous MoS_2 according to the equation 2.1. The supersaturated MoS_2 vapor and sub-oxide compounds vapor facilitate the growth of vertically oriented MoS_2 due to higher diffusion rate and high density of nucleation sites of MoS_2 on Si [134]. The merger of two MoS_2 islands leads to the intensive compression which forces the distortion to form arch structure to release the pressure and result in the vertical growth of MoS_2 on Si substrate as shown schematically in **Figure 2.5**.

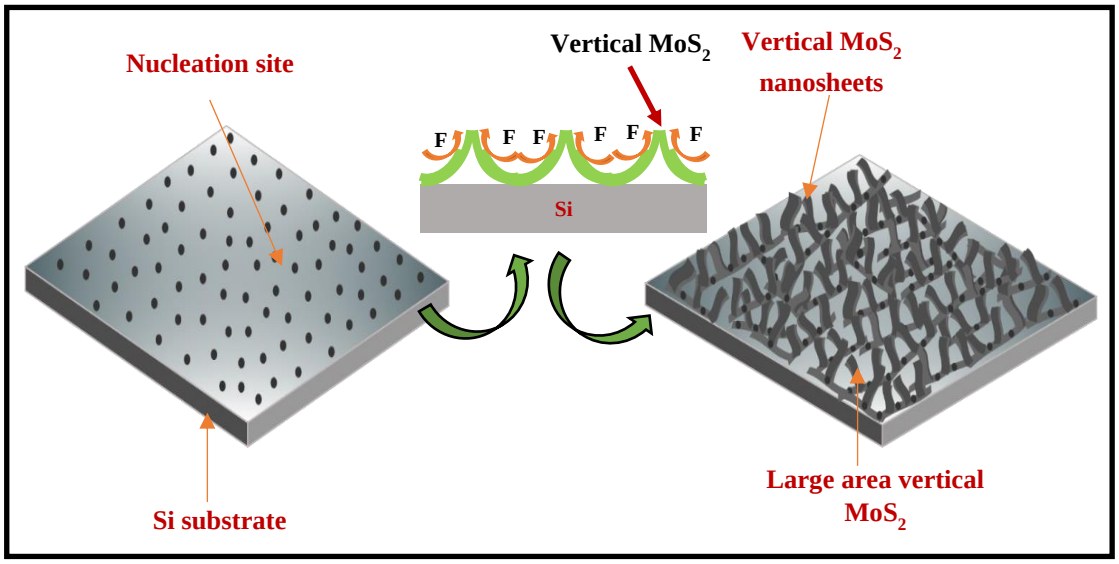

Figure 2.5 *Schematic diagram of growth mechanism of vertically oriented few-layer MoS_2 nanostructure over Si substrate.*

These three prepared MoS_2 nanostructures were characterized by different characterization technique to understand their morphologies and physical properties such as thermal conductivity, tunable bandgap. Their photodetection and SERS applications have been investigated. The following section deals with different characterization tools used in this work.

2.2Characterization Techniques

The prepared different MoS_2 samples have been characterized by different characterizations tools to confirm the structural, morphological and optical properties.

The different characterization techniques, used in the present thesis, are briefly discussed below.

2.2.1 X-ray Diffraction (XRD)

X-ray diffraction (XRD) is a non-destructive technique used to identify the structural properties of materials. In this characterization technique, an electromagnetic wave of wavelength of ~1 Å is diffracted from the crystal lattice planes oriented in distinct directions in crystal due to comparable order of magnitude of the X-rays wavelength and crystal lattice. The X-ray diffractometer consists of three basic components-

a) X-ray tube
b) A sample holder
c) X-ray detector

X-rays are generated in a cathode ray tube (CRT) by heating a filament to generate electrons. These electrons are accelerated by applying voltage and having certain energy to eject out the inner shell electrons of the target. During that time the characteristic X-rays are generated from the target having different components K_α and K_β. The K_α consists of two wavelengths, $K_{\alpha1}$ and $K_{\alpha2}$. $K_{\alpha1}$ has a slightly shorter wavelength and double the intensity as $K_{\alpha2}$. The filter is used to produce the monochromatic X-ray. The XRD works on the principle of Bragg's law, which suggests that a constructive interference will be resulting in an intense peak when the path difference between the waves is an integral multiple of the X-ray wavelength. The Bragg's law can be expressed as follows-

$$2d_{hkl}\mathrm{Sin}\theta = n\lambda \qquad (2.3)$$

where, the interplanar distance is d_{hkl} (h, k, l are Miller indices) and θ represents the Bragg's angle [135,136]. The order of diffraction is n (n = 1 for XRD) and λ is the wavelength of the X-Ray. **Figure 2.6** is the illustration of the Bragg‘s law. The diffraction peaks depend upon the symmetry of the structure of the materials.

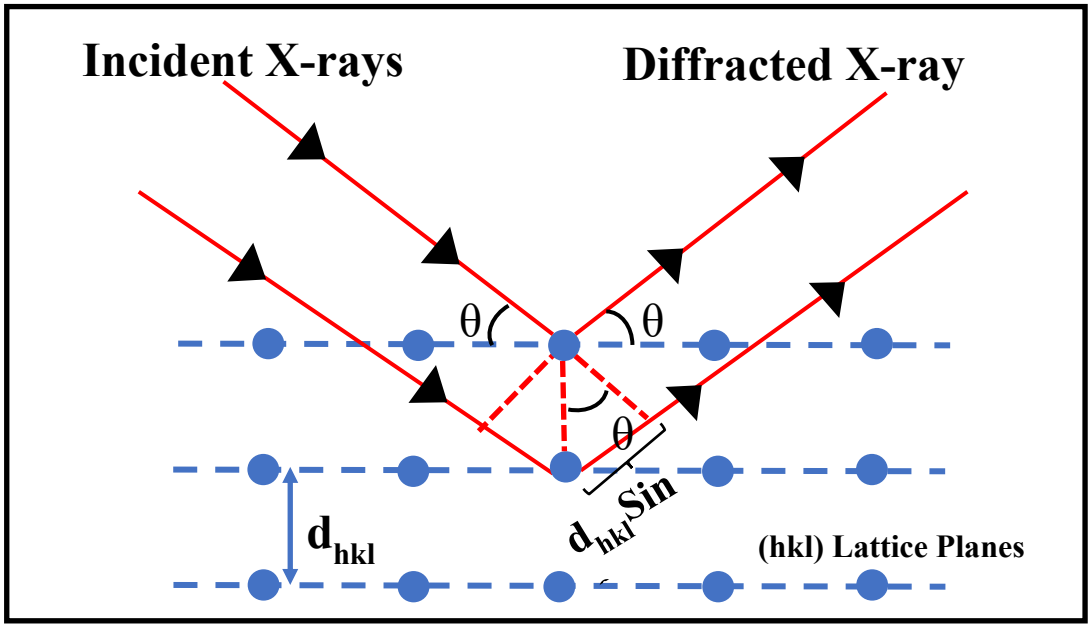

Figure 2.6 *Schematic diagram of incident and diffracted X-rays from the crystal.*

2.2.2 Scanning Electron Microscope (SEM)

Electron microscopy has been a revolutionary imaging technology widely used by the scientific and engineering community to observe the morphology and structure of nanomaterials. The Nova NanoSEM 450 scanning electron microscope (SEM) was employed to understand the morphology of the prepared sample. In SEM technique, an electron beam is focused with the help of different magnetic lens and apertures on the sample to create an image. In this measurement technique the specimen needs to be electronically conducting to avoid the charging effects, which produce blur image quality at high resolutions. **Figure 2.7** shows the typical layout of SEM, which consists of electron gun from where the electrons are generated and accelerated via accelerating

anode, electromagnetic lenses for focussing the electrons, a vacuum chamber and detector to collect the signals emitted from materials [137]. The scattering occurs due to interaction between the high energy electrons and the specimen, which results in generation of different signals such as secondary electrons, backscattered electrons, characteristic X-rays and auger electrons. The auger electrons are generated from the surface of the sample in low atomic number molecule. The secondary electrons are generated by the inelastic scattering and they have energy around few keV and backscattered electrons are generated by elastic scattering and having high energy. The imaging is done with improved spatial resolution by the secondary electron [137, 138]. The image quality in SEM depends on the depth of field and the resolution, which can be affected by working distance, probe current, accelerating voltage and astigmatism. The resolution in SEM is in the nano-meter range.

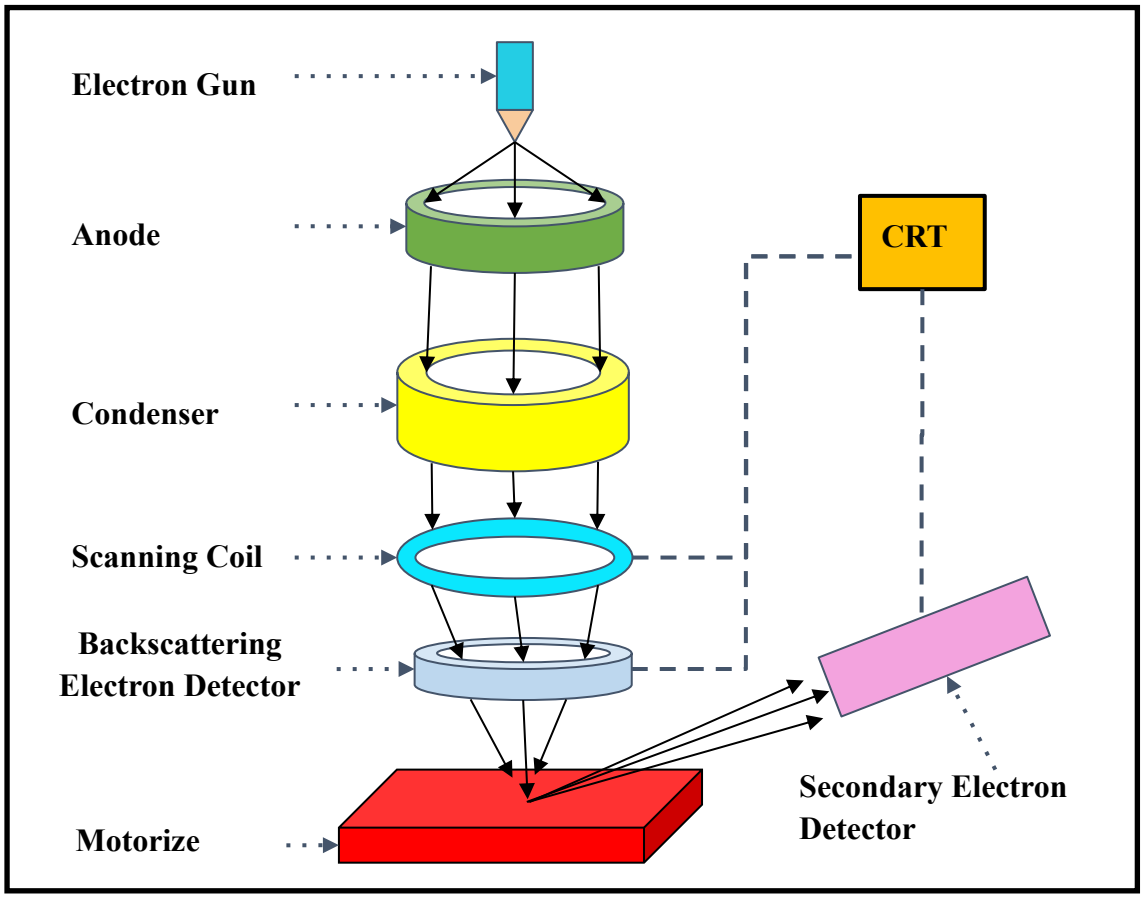

Figure 2.7 *Schematic diagram of core component of SEM microscope [138].*

2.2.3 Transmission Electron Microscope (TEM)

Transmission electron microscopy (TEM) has been widely used to characterize nanomaterials. It is an electron microscopy technique, where the incident electron beam is transmitted through the material to generate a two-dimensional (2D) image. The FEI Tecnai G2 20 TWIN TEM was employed to observe the thickness and the selective area electron diffraction (SAED) pattern of the prepared sample. In TEM, like SEM, an electron beam is focused with the help of different magnetic lens and apertures on the sample. However, in TEM, electrons are transmitted through the specimen and they arrive at a detector below the sample to produce 2D image of the specimen. This image gives the detail information of sample's morphology, composition and the crystal structure [138,139]. The typical layout of TEM is shown in **Figure 2.8 (a)**, where the objective aperture is placed in the back focal plane of the objective lens. Transmitted and diffracted electrons are used by changing the aperture position for the bright-field and dark-field imaging modes in TEM as shown in **Figure 2.8 (b)** and **Figure 2.8 (c),** respectively. The transmitted electrons can pass through the aperture in bright-field mode and the obtained images depict mass-thickness contrast. However, in the dark-field mode, the transmitted electrons are fully blocked by aperture and diffracted electron beam is allowed to pass through the aperture, which provides the information about the crystal structure [138,140]. In TEM, the specimen needs to be ultrathin (less than 100 nm) or a suspension of the material on a grid. The TEM has the highest resolution (atomic level) of any electron microscope and it has magnification 10 to 50 million times.

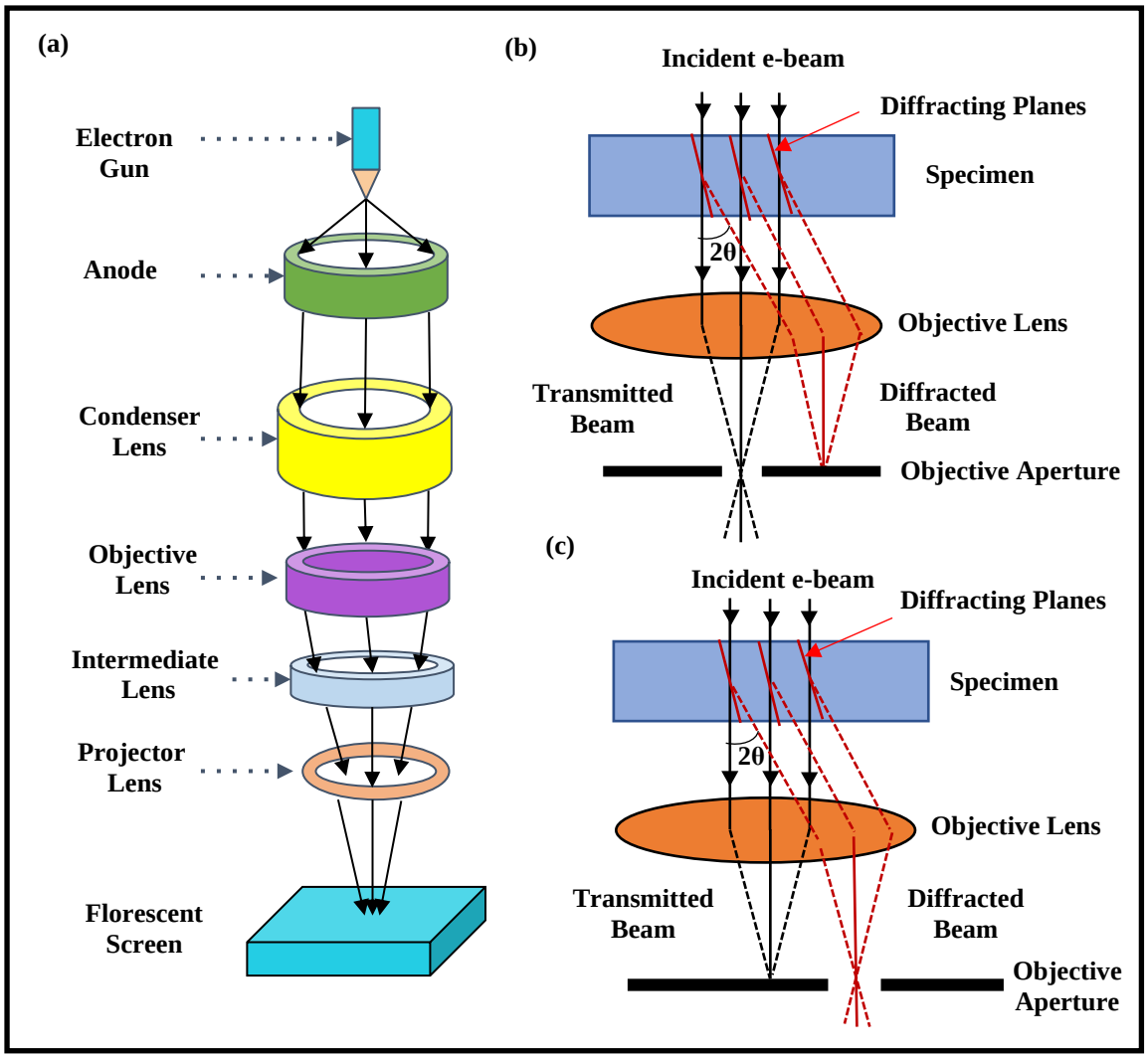

Figure 2.8 *(a) Schematic diagram of core component of TEM microscope. Transmitted and diffracted electrons for (b) Bright field and (c) Dark field imaging in TEM [138].*

2.2.4 Atomic Force Microscopy (AFM)

Atomic force microscopy (AFM) is a powerful technique that has been widely used to image surface of a specimen. Modern AFM provides a general method for doing non-destructive surface profilometry at a resolution better than 1 nm and perhaps down to the atomic level. It senses very low amount force of (10^{-2} to 10^{-8} N) between the tip and the specimen surface as a function of distance. The schematic diagram of the atomic force microscope is shown in **Figure 2.9**. The basic components of an AFM are probe, cantilever, laser, a data processor and a photodetector. A sharp V-shaped probe is

mounted at the end of a flexible microcantilever arm [141]. The probes and cantilevers are mostly made of silicon nitride or silicon due to high stability of their mechanical properties and the top surface of the cantilever is coated with a thin reflective material, typically made of either gold or aluminium. A beam of laser light falls on the cantilever and reflects back onto a position-sensitive photodetector. Any deflection of the cantilever creates a change in the position of the laser spot on the photodetector, which can be monitored [142]. The probe can be raster-scanned across the surface of the specimen and a 3D image i.e., the relative height information of the sample can be built.

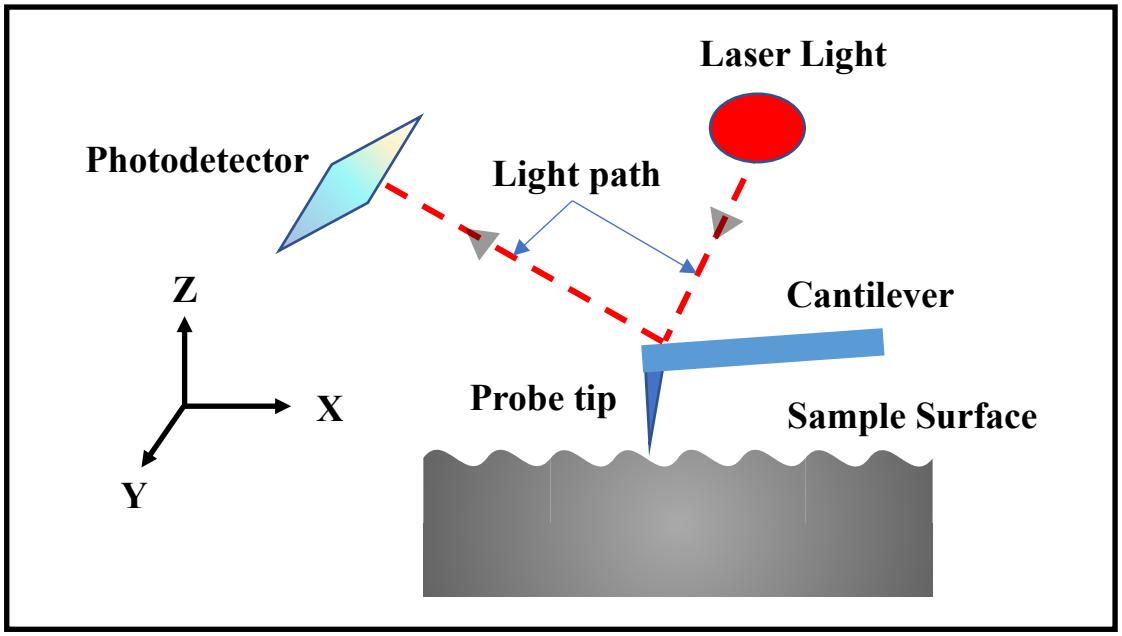

Figure 2.9 *Schematic diagram of the atomic force microscope [141].*

2.2.5 Raman Spectroscopy

Raman spectroscopy is a non-destructive powerful tool to characterize 2D materials, like graphene and transition metal dichalcogenides [30, 35]. Raman spectroscopy has been widely used to figure out the layer number and the defect in 2D materials. The basic principle of Raman spectroscopy is based on the interaction between electromagnetic field (EMF) and materials/molecules, which results in inelastic

scattering. The incident EMF i.e. photons interact with the analyte molecule, and a dipole moment is induced which is directly proportional to the polarizability of the molecule. The magnitude of induced dipole moment (μ_{ind}) depends on the strength of the incident electric field (E_{in}) and the polarizability of the molecule (α_m) and it can be expressed as follows [23]

$$\mu_{ind} = E_{in}(\omega_{inc}).\alpha_m \tag{2.4}$$

In the Raman scattering process, the incoming photons are not absorbed by the molecule rather they are scattered. The scattered photon frequency is proportional to the difference in energy of the molecular vibrational levels. The classical theory explained the inelastic scattering of incident electric field E_{in} and the angular eigen frequency (ω_{vib}) of the vibrating molecule. This interaction results in three dipole components $\mu_{ind}(\omega_{inc})$, $\mu_{ind}(\omega_{inc} - \omega_{vib})$ and $\mu_{ind}(\omega_{inc} + \omega_{vib})$ corresponding to Rayleigh, Stokes and Anti-Stokes, respectively, as shown in **Figure 2.10**. [23, 119, 143]

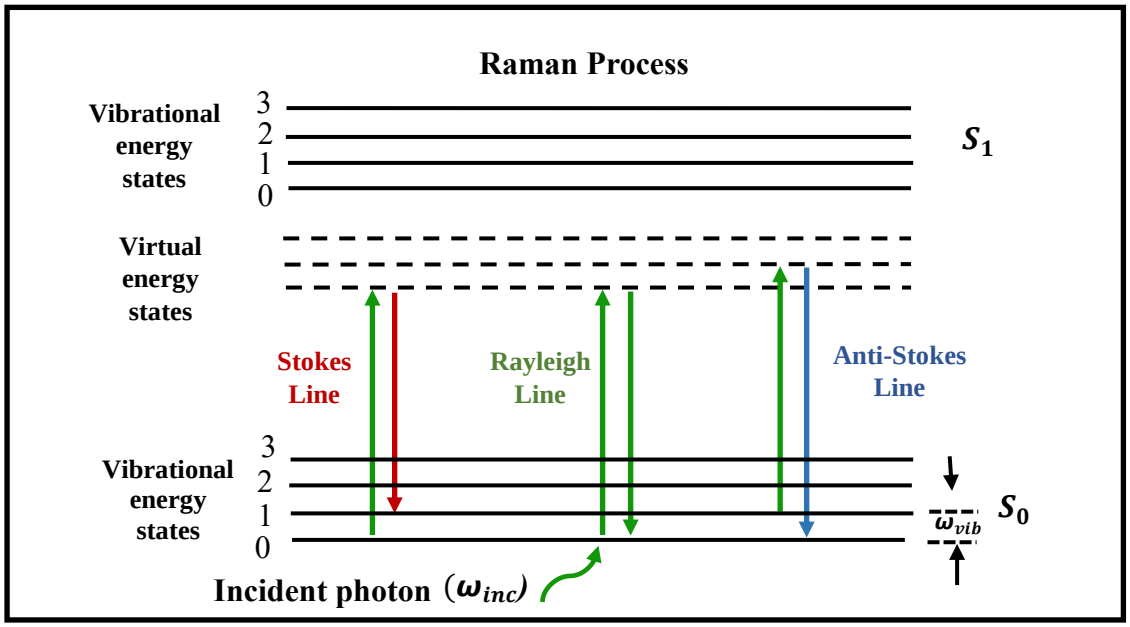

Figure 2.10 *Schematic representation of the scattering process in Raman scattering (Rayleigh, stokes and anti-stokes line) [119].*

The shorter wavelength laser possesses higher Raman scattering (inelastic scattering) cross-sections; hence it provides greater signal. In Raman study the inelastic scattering occurs when the incident photon wavelength is different from the scattered photon wavelength, the higher wavelength is stokes and the lower wavelength is the anti-stokes lines. The intensity of the Raman signal is very weak as compared to the incident laser, i.e., single inelastic scattering out of one million scatterings. In the present work, the vibrational characteristics of prepared MoS_2 nanostructures was characterized by STR-300 micro-Raman spectrometer with a solid-state green laser having excitation wavelength of 532 nm. A Raman spectrometer has mainly three components such as laser, the sampling interface and spectrometer as shown schematically in **Figure 2.11**. In our Raman system, fiber optics cables have been used to transmit and collect the signal from the specimen. To remove the Rayleigh signals, a notch filter is used and the remaining signals are passed through a dispersive holographic grating. To reduce the intensity of the incident monochromatic laser source, we have used different neutral density filter. To detect the Raman signal, a high-quality CCD detector is used.

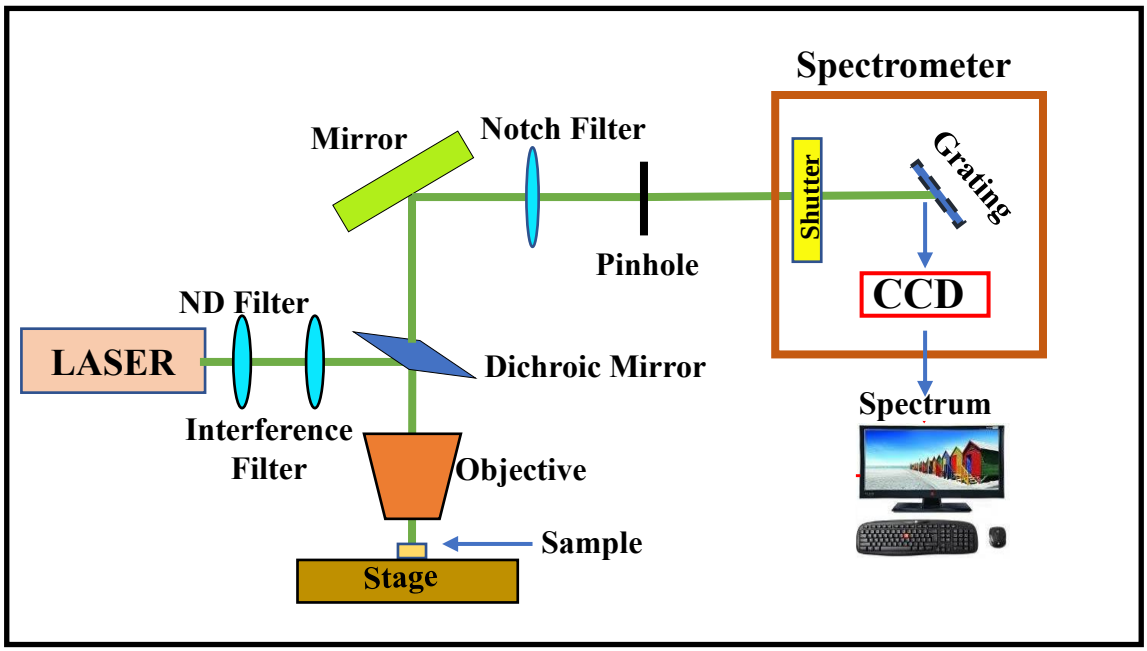

Figure 2.11 *Schematic diagram of Raman spectrometer.*

2.2.6 Photoluminescence (PL) Spectroscopy

Photoluminescence (PL) is a non-destructive, contactless and highly sensitive technique, which has been widely used to analyze the semiconducting nature of materials. In this process electron-hole pairs (excitons) are generated due to the coulomb interaction upon optical excitation of light. When the excited electrons come to ground or lower energy states can either emit light (radiative process) or may not emit light which is known as the non-radiative process. The radiative emission is known as photoluminescence (PL). The wavelength of the emitted signal is equal to the energy difference between final (excited) and initial (ground state) energy levels of the contributing electrons. The schematic diagram of PL is shown in the **Figure 2.12**. The electron excited by the incident photons from the ground state S_0 to the excited state S_1. Then these excited electrons are relaxed to the lowest energy of the excited state (S_1) via a series of non-radiative transitions as shown in **Figure 2.12**. Finally, these electrons are relaxed to ground state (S_0) via emission of photon having lower energy (longer wavelength) than the excitation photon [6,119,144]. For the PL measurement of prepared MoS_2 nanostructures, we have used the same system (set of excitation laser source, spectrometer and CCD detector), which has been used in Raman study.

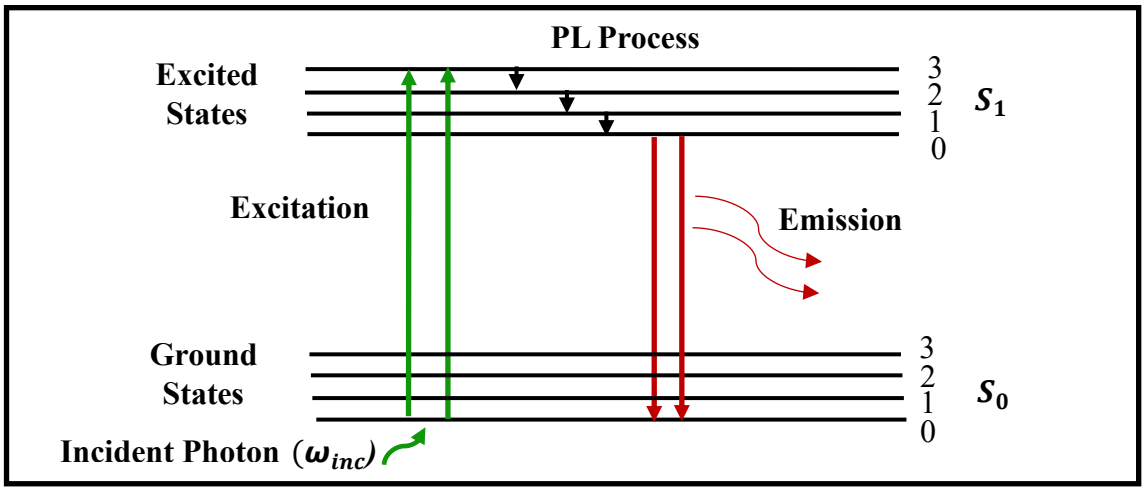

Figure 2.12 *Schematic representation of the photoluminescence spectroscopy [119].*

2.2.7 UV-Visible Spectrophotometer

This is a useful technique to determine the band gap and the absorption properties of materials with in the visible and adjacent (near-ultraviolet and near-infrared) range. A compound absorbs light in the UV-visible region and get excited and the absorption spectra is used to determine the bandgap of the semiconductors. The absorbance is measured with respect to a reference and a graph of absorbance vs wavelength is plotted [145]. The schematic diagram of UV-visible spectrophotometer is shown in **Figure 2.13**. In this study difference between absorbed light intensities of sample and reference cell is measured to identify the absorption characteristic of the sample.

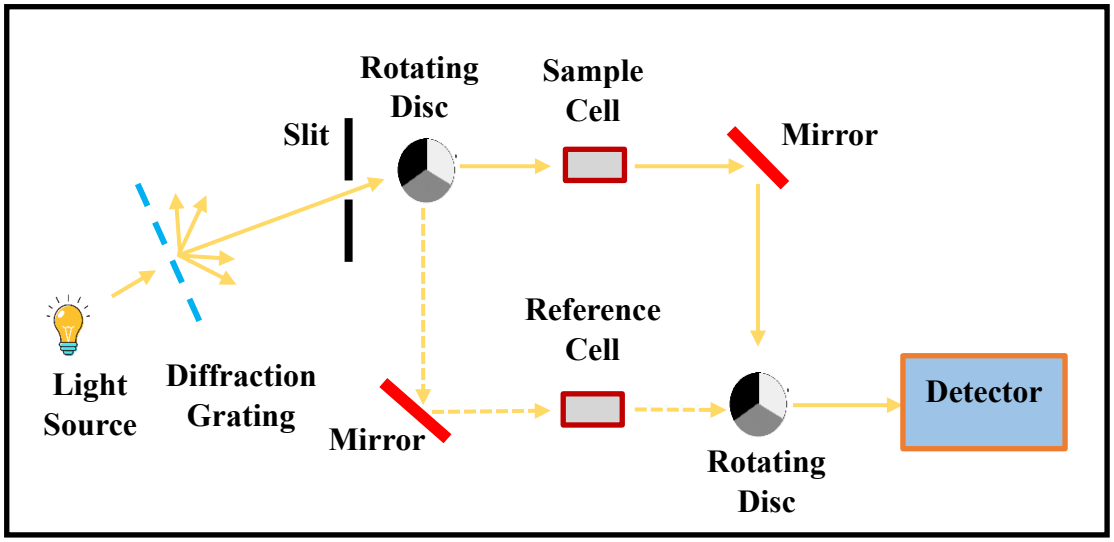

Figure 2.13 *Schematic diagram of UV-Visible spectrometer [145].*

2.2.8 Current Voltage (IV) Measurement

The current-voltage (I-V) characteristic curve is a graphical representation of the relationship between the potential applied across a device and the current flowing through it. The I-V curves represent the characteristic behaviour of electronic devices as their shape varies for different devices such as resistor, diode, solar cell etc. The characteristics I-V measurements for photodetection study have been performed using Autolab

instrument (model no. PGSTAT204). The I-V measurement is performed by applying a series of potential to device and at the same time the current flowing through the device is recorded at each voltage.

2.2.9 SERS Measurement

As an advanced approach to Raman spectroscopy, Surface enhanced Raman spectroscopy (SERS) is known to be a powerful tool in detecting molecules at very low concentration level. In order to improve the Raman signal, interaction between probe molecules and SERS substrate is utilised [110]. Depending upon the type of substrate, metallic and semiconducting substrates, signal enhancement is obtained due to the plasmon resonance or chemical enhancement, respectively. In the present work, SERS study has been performed using STR300 Raman spectrometer and prepared semiconducting MoS_2 nanostructures as active substrates. In this process, different concentrations of dye solutions were prepared by serial dilution process and active SERS substrates were prepared by solution soaking process.